Biochimica et Biophysica Acta 1838 (2014) 164–172

Contents lists available at ScienceDirect

Biochimica et Biophysica Acta

journal homepage: www.elsevier.com/locate/bbamem

NMR-based approach to measure the free energy of transmembrane helix–helix interactions

Konstantin S. Mineev [a,*,1], Dmitry M. Lesovoy [a,1], Dinara R. Usmanova [a,b], Sergey A. Goncharuk [a,c], Mikhail A. Shulepko [a,c], Ekaterina N. Lyukmanova [a], Mikhail P. Kirpichnikov [a,c], Eduard V. Bocharov [a], Alexander S. Arseniev [a]

[a] Shemyakin–Ovchinnikov Institute of Bioorganic Chemistry RAS, Str. Miklukho-Maklaya, 16/10, Moscow 117997, Russian Federation
[b] Moscow Institute of Physics and Technology, Institutsky per., 9, Dolgoprudny 141700, Russian Federation
[c] Lomonosov Moscow State University, Moscow 119991, Russian Federation

ARTICLE INFO

Article history:
Received 22 May 2013
Received in revised form 27 August 2013
Accepted 30 August 2013
Available online 10 September 2013

Keywords:
NMR spectroscopy
Dimerization
Transmembrane helix
Free energy
Detergent micelle

ABSTRACT

Knowledge of the energetic parameters of transmembrane helix–helix interactions is necessary for the establishment of a structure–energy relationship for α-helical membrane domains. A number of techniques have been developed to measure the free energies of dimerization and oligomerization of transmembrane α-helices, and all of these have their advantages and drawbacks. In this study we propose a methodology to determine the magnitudes of the free energy of interactions between transmembrane helices in detergent micelles. The suggested approach employs solution nuclear magnetic resonance (NMR) spectroscopy to determine the population of the oligomeric states of the transmembrane domains and introduces a new formalism to describe the oligomerization equilibrium, which is based on the assumption that both the dimerization of the transmembrane domains and the dissociation of the dimer can occur only upon the collision of detergent micelles. The technique has three major advantages compared with other existing approaches: it may be used to analyze both weak and relatively strong dimerization/oligomerization processes, it works well for the analysis of complex equilibria, e.g. when monomer, dimer and high-order oligomer populations are simultaneously present in the solution, and it can simultaneously yield both structural and energetic characteristics of the helix–helix interaction under study. The proposed methodology was applied to investigate the oligomerization process of transmembrane domains of fibroblast growth factor receptor 3 (FGFR3) and vascular endothelium growth factor receptor 2 (VEGFR2), and allowed the measurement of the free energy of dimerization of both of these objects. In addition the proposed method was able to describe the multi-state oligomerization process of the VEGFR2 transmembrane domain.

1. Introduction

The behavior of integral membrane proteins to a great extent depends on the interactions between the transmembrane (TM) α-helices inside their membrane domains. Most of all these interactions are significant for the processes of activation and signal transduction in dimeric bitopic integral membrane proteins, such as receptor tyrosine kinases [1]. Moreover, the dimeric TM domains (TMDs) of bitopic membrane proteins represent the simplest and most convenient model to investigate the basic principles of helix–helix interactions inside the membrane-like environment provided by the detergent micelles or lipidic bicelles, which are the most appropriate membrane mimetics for studying both the structural parameters and free energy of the association of TM α-helices. Over the past ten years a lot of effort was made to understand the structural basis of the dimerization of single-span TM domains [2–7]. These studies led to a number of atomic spatial structures of α-helical TM dimers, which allowed the determination of several sequence motifs that are involved in the TM helix–helix interaction. To obtain the full structural and thermodynamic image of the helical TM domain, to provide a realistic model of its behavior, and to predict and understand the effects of various factors, such as single point mutations and a lipidic environment, the relationship between the structural properties and the free energy associated with a TM helix–helix interaction needs to be established. Thus, it is necessary to develop a reliable and accurate method for measuring the free energy and other thermodynamic parameters of the association of TM helices

Abbreviations: NMR, nuclear magnetic resonance; DPC, dodecylphosphocholine; TM, transmembrane; TMD, transmembrane domain; LPR, lipid to protein ratio; CMC, critical micelle concentration; FRET, Forster resonance energy transfer; FGFR3, fibroblast growth factor receptor 3; VEGFR2, vascular endothelium growth factor receptor 2; FGFR3tm, TM domain of FGFR3; VEGFR2tm, TM domain of VEGFR2 bearing $V^{769}E$ substitution; TROSY, transverse relaxation optimized spectroscopy; HSQC, heteronuclear single quantum coherence; SDS-PAGE, sodium dodecyl sulfate polyacrylamide gel electrophoresis; TFE, trifluoroethanol; TSP, trimethylsilyl propanoic acid; TCEP, tris(2-carboxyethyl)phosphine; CECF, continuous exchange cell-free

* Corresponding author at: Str. Mikluho-Maklaya, 16/10, Moscow 117997, Russian Federation. Tel.: +7 495 330 74 83.
E-mail address: mineev@nmr.ru (K.S. Mineev).

[1] Konstantin S. Mineev and Dmitry M. Lesovoy contributed equally to this work.

0005-2736/$ – see front matter © 2013 Elsevier B.V. All rights reserved.
http://dx.doi.org/10.1016/j.bbamem.2013.08.021

A number of approaches have been developed for and successfully applied to the investigation of the processes of oligomerization in detergent micelles: gel electrophoresis [8], sedimentation equilibrium [9,10], genetic assays (ToxR, ToxCat) [11,12] and FRET [13]. All of these approaches have their advantages and drawbacks. Excluding the Tox systems and SDS-PAGE, which do not yield the free energy and provide only qualitative data, the two other approaches have two major disadvantages. First, they cannot be used to analyze a weakly dimerizing system because they cannot distinguish between the specific dimerization and the co-localization of TMDs induced by a low lipid-to-protein ratio. Second, FRET (but not analytical ultracentrifugation) cannot work properly under a complex multistate equilibrium, i.e. when the TM helix exists simultaneously in several states, such as monomer, dimer, trimer and tetramer. In contrast, NMR spectroscopy allows one to directly measure the population of states when the transitions between different oligomeric forms of the TM domain are slow (which is the common case for TM helix dimerization). That is, NMR spectroscopy can be used to detect the monomeric form of the protein even if several monomers are located close to each other (e.g. within the same micelle), and to detect the population of all oligomeric states of the TM helix separately and through a single experiment. Additionally, in contrast to FRET spectroscopy in liposomes, NMR spectroscopy in micelles can provide data on both the structural properties and the energy of helix–helix interaction simultaneously, sometimes through the same experiment. Thus, NMR spectroscopy may be considered a powerful instrument for the study of both the energetic and the structural properties of TM helix–helix interactions inside the membrane domains. Recently, the use of NMR spectroscopy to distinguish between specific and non-specific helix–helix interactions in detergent micelles was suggested for the fast dimer–monomer transitions of the helical TM domains [14]. In our previous studies [15,16] we have performed helix–helix dimerization free energy measurements by means of NMR spectroscopy in micelles and bicelles, but our analyses were hindered by the nonideal behavior of the system at a low lipid-to-protein ratio. In the present work, we describe a new methodology and formalism for free energy measurements conducted in detergent micelles, which is applicable to both strongly and weakly dimerizing TM domains and does not suffer from the difficulties associated with the interpretation of the results obtained at a low lipid-to-protein ratio. The technique was verified using the TM domain of FGFR3 (weakly dimerizing TM domain) and a mutant TM domain of VEGFR2 (V769/E), which is capable of forming stable dimers and trimers.

2. Materials and methods

2.1. Protein expression, purification and sample preparation

The gene encoding the 37-residue mutant VEGFR2 fragment 759–795 (ME^{759}KTNLEIIILEGTAVIAMFFWLLLVIILRTVKRANGG^{795}, VEGFR2tm, the theoretically predicted TM α-helix is underlined), including the hydrophobic TM segment flanked by polar N- and C-terminal regions, the N-terminal Met residue, and the V^{769}E substitution, was amplified using PCR and cloned into the pET-22b(+) vector (Novagen, USA) using the NdeI and BamHI restriction sites. The resulting plasmid pET-22b(+)/TM-VEGFR2 was used as a template in a bacterial continuous exchange cell-free (CECF) expression system. The ^{13}C,^{15}N-labeled protein was expressed in the CECF system using previously described protocols [17] without the addition of any membrane-mimicking media and with the addition of an algal mixture of ^{13}C, ^{15}N -enriched amino acids (Isotec™), ^{13}C, ^{15}N -tryptophan, and ^{13}C, ^{15}N -asparagine at concentrations of 3.7 mg/ml, 2.3 mM, and 1.3 mM, respectively.

The VEGFR2tm samples were prepared from the reaction mixture precipitate by solubilization with a TFE/H_2O (2:1) mixture containing 1 mM TSP. The quality of the sample and the concentration of the peptide were controlled by 1D NMR spectroscopy. Then, 500 μl of the H_2O/TFE (2:1) solution containing 0.65 mM ^{13}C,^{15}N-labeled VEGFR2tm was centrifuged, lyophilized, and then dissolved in 500 μl of a 90 mM DPC-d_{38} (Cambridge Isotope Laboratories, USA) aqueous solution containing 20 mM deuterated sodium acetate and 1 mM NaN_3. An ultrasonic bath and Vortex shaker were used for the sample homogenization, and the pH was adjusted to 4.5. DPC-d_{38} was added to the initial volume from 10- to 40-μl aliquots of the 200 mg/ml stock solution for the measurement of the dependence of the VEGFR2tm dimer dissociation constant on the detergent concentration. To ensure a homogeneous and equilibrium distribution of the peptide among the micelles, the mixture was subsequently subjected to 3–4 freeze–thaw cycles and a 30- to 40-min stabilization at 45 °C in the NMR spectrometer. When the concentration of DPC reached 10%, the sample was 3-fold diluted with a 1 mM solution of DPC, and 450 μl of the resultant solution was used for further detergent addition. At each concentration, the 2D ^{15}N,^{1}H-TROSY-HSQC spectrum [18] was recorded. At some concentrations, several spectra were acquired to reduce the errors and obtain better statistics. In total, 29 NMR spectra at 17 different DPC concentrations and detergent-to-protein ratios were obtained.

The ^{15}N-labeled sample of the recombinant 43-residue peptide FGFR3tm(L^{357}PAEEELVEADEAGSVYAGILSYGVGFFLFILVVAAVTLCRLR^{399}, FGFR3tm, the predicted TM segment is underlined) was produced in *Escherichia coli* and purified as previously described [19]. The peptide powder was first dissolved in a 7:3 (v/v) trifluoroethanol–water mixture with the addition of a 9:1 (mol/mol) mixture of deuterated DPC (d_{38}, 98%, CIL) and SDS (d_{29}, 98%, CIL). The samples were placed for several minutes in an ultrasound bath and then lyophilized. The dried ^{15}N-labeled and "isotopic heterodimer" samples were dissolved at pH 5.7 in 300 μl of buffer solution containing 5 mM citric acid, 15 mM Na_2HPO4, 6 mM TCEP, 0.3 mM sodium azide, and 5% D_2O (v/v). TCEP was used to prevent the formation of a possible intermolecular S–S bridge between the naturally occurring N-terminal Cys^{396} residues, which do not participate in the FGFR3 TM domain dimerization [20]. To ensure uniformity of the micelle size, the sample was subjected to several freeze–thaw cycles (heating to 40–45 °C) and then sonication until the sample became transparent. The self-association and the monomer–dimer transition of FGFR3tm were studied as the lipid-to-protein molar ratio (LPR) was varied within the range of 30 to 520.

2.2. NMR spectroscopy

The NMR spectra were acquired on an 800-MHz Bruker Avance III spectrometer (Bruker Biospin Gmbh, Germany) equipped with cryogenic probe either at 45 °C (VEGFR2tm) or at 40 °C (FGFR3tm). The correlation times of the rotational diffusion of the amide groups were measured through TROSY-based experiments, as described previously [21].

2.3. Measurement of the oligomeric state populations

The populations of oligomeric states were reconstructed from the intensities of the cross-peaks in the TROSY spectra by taking into account the proton transverse relaxation rates (R_2) and the duration of the polarization transfer steps in the NMR pulse sequence. For 25 different cross-peaks in the NMR spectrum of VEGFR2tm, which can be integrated separately and correspond to different oligomeric states, the R_2 and intensities (I) were measured through lineshape analysis. To measure the R_2, the ^{15}N-TROSY-HSQC spectra were processed with an exponential apodization function, and 1D slices were fitted with lorentzian lineshapes using the Wolfram Mathematica software. The intensities of the 2D cross-peaks in the NMR spectra were determined through a two-dimensional approximation of the cross-peaks in the spectra, which were processed using the Gaussian apodization function. The dependence of I on R2 was fitted with either a monoexponential decay function

$$I = I_0 \exp\left[-\alpha R_2 t_\Sigma\right], \quad (1)$$

where I_0 is the reconstructed intensity, R_2 is the measured proton transverse relaxation rate, α is a fitted parameter, and t_Σ is the sum of the durations of the transfer steps, or a more complex model

$$I = I_0 \exp[-\alpha R_2 t_1 - R_2 t_3] \cdot (0.25 + 0.5 \exp[-\alpha R_2 t_2] + 0.25 \exp[-2\alpha R_2 t_2], \quad (2)$$

where all of the parameters are the same as in Eq. (1) with the exception of t_1, t_2, and t_3, which are the durations of the first INEPT, the back-INEPTs, and the gradient echo steps in the TROSY pulse sequence [18]. The first model assumes that the whole magnetization decays with effective rate αR_2, and the second considers the evolution of all of the terms relaxing during the pulse sequence when protons are in the transverse plane, neglects the nitrogen relaxation, and presumes that the density matrix elements, evolving during the transfer periods, relax with effective rate αR_2. Three sets of data points, which correspond to the monomeric, dimeric, and oligomeric states, were approximated by Eqs. (1) or (2) with the same parameter α. The fitted curves are shown in Fig. 1C. Both models were in good agreement with the experimental data and yielded a nearly identical monomer/dimer/oligomer ratio. We therefore selected the simplest one for further calculations. This procedure was performed for all of the acquired spectra because the parameters of the model depend on the magnetic field inhomogeneity and on the solution viscosity. The NMR spectra of FGFR3tm were treated analogously.

2.4. Determination of monomer, dimer and oligomer concentrations

The obtained populations of states were used to calculate the concentrations of monomers and dimers of the TM domain in solution:

$$[M] = [P]p_m/(p_m + p_d),$$

$[D] = [P]p_d/2(p_m + p_d)$, where [P] is the concentration of the peptide and p_m and p_d are the populations of the monomeric and dimeric states, correspondingly.

In the case in which the third oligomeric state was present in the solution, the concentrations of monomers and dimers were calculated using different formulae:

$$[M] = [P]p_m/(p_m + p_d + p_O),$$

$[D] = [P]p_d/2(p_m + p_d + p_O)$, where [P] is the concentration of the peptide and p_m, p_d, and p_o are the populations of monomeric, dimeric, and trimeric states, respectively.

The concentration of the oligomeric state [O] was calculated depending on the model and was assumed to be in oligomerization equilibrium:

$$[O] = [P]p_o/n \cdot (p_m + p_d + p_O),$$

where n is the oligomeric number of state O.

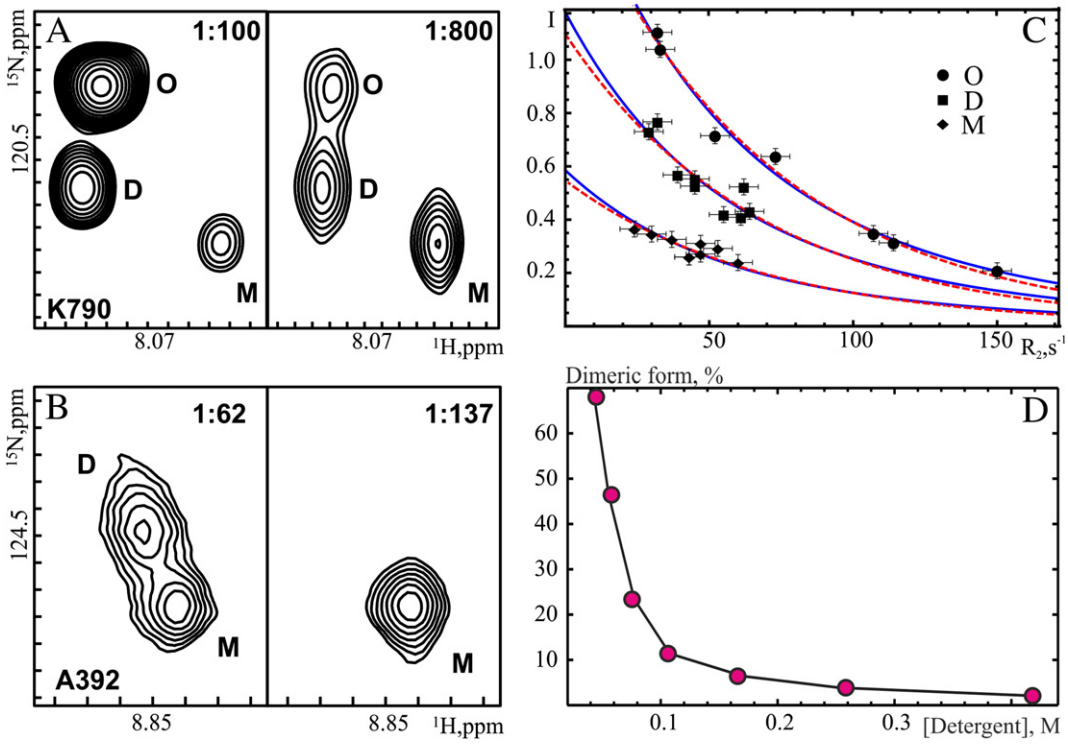

Fig. 1. (A) — Fragments of the $^1H,^{15}N$-TROSY-HSQC spectrum of VEGFR2tm acquired at LPRs of 100 and 800. The cross-peaks that correspond to the NH group of K790 and originate from the monomeric (M), dimeric (D), and oligomeric (O) states of VEGFR2tm are shown. (B) — Fragments of the $^1H,^{15}N$-TROSY-HSQC spectrum of FGFR3tm acquired at LPRs of 62 and 137. The cross-peaks that correspond to the NH group of A392 and originate from the monomeric (M) and dimeric (D) states of FGFR3tm are shown. (C) — Dependence of the 2D cross-peak intensity in the $^1H,^{15}N$-TROSY-HSQC spectra of VEGFR2tm on the amide proton transverse relaxation rate. Three sets of peaks, which correspond to the monomeric (rhomboids), dimeric (squares) and oligomeric (circles) forms of VEGFR2tm, are shown. The dashed and solid lines represent the fitted curves for monoexponential decay (1) and complex model (2), respectively. The spectra were acquired for a 0.6 mM sample of VEGFR2tm at a DPC-to-protein ratio of 200 and a temperature of 45 °C. (D) — Percentage of the dimeric form of FGFR3tm as a function of the detergent concentration. The experimental values (circles) were calculated from the cross-peak intensities in the $^1H,^{15}N$-TROSY-HSQC spectra. The spectra were acquired for a 0.8 mM sample of FGFR3tm at 40 °C. The theoretical values (dashed line) were obtained through approximation of the experimental data by Eq. (7); the approximation parameters N_e, N_m, N_d, and K_{eq} were found to be 50 ± 2, 76 ± 7, 102 ± 10, and 0.1 ± 0.02, respectively.

Here and further in the text standard molar concentration units (moles of the substance per liter of solution) are used for the protein and detergent.

3. Theory

The present study was dedicated to the development of a methodology for the measurement of the free energy of dimerization and oligomerization of TM α-helices. As the model objects, we selected two different TMDs of receptor tyrosine kinases: FGFR3tm, which forms a weak dimer in DPC micelles, and mutant VEGFR2tm, which is able to form two different stable oligomeric forms even at excess amounts of detergent. The conclusion on the oligomerization propensity of the objects under investigation was made through an analysis of the NMR spectra at different lipid-to-protein ratios (LPRs) and different NMR rotational correlation times measured for the cross-peaks, which correspond to the different states.

To determine the free energy of interaction between the TMDs in DPC micelles, it is necessary to suggest an appropriate physical model for the oligomerization process occurring in detergent micelles. Previously, two different models were considered to describe the dimerization of glycophorin A and PON1 [13,22–24]. The first model states that the detergent acts as a solvent in the dimerization process (Fig. 2A), and we denoted this model the "continuous solvent" model. In this model, the kinetics of the dimer–monomer transition depend on the monomer-to-detergent and the dimer-to-detergent ratios and not on the molar monomer and dimer concentrations measured with respect to the volume of the water solution. The idea to use the molar or volume fraction units rather than the absolute molar concentrations to study the interactions of membrane associated-molecules was expressed in early studies of the phospholipase A2 kinetics [25,26] and was later applied to the measurement of the free energy for the interaction of the glycophorin A TM segments in micelles [24] and EGFR TMDs in liposomes [27]. In the "continuous solvent" model, the rates of the processes and the equilibrium constants have the following form:

$$V_{dim} = k_{dim}\left(\frac{[M]}{[Det]}\right)^2 \tag{3}$$

$$V_{dis} = k_{dis}\frac{[D]}{[Det]} \tag{4}$$

$$K_{eq} = \frac{[M]^2}{[D]\cdot[Det]} \tag{5}$$

where V_{dim} and V_{dis} are the rates of dimerization and dissociation, respectively, k_{dim} and k_{dis} are the rate constants of dimerization and dissociation, respectively, [M], [D], and [Det] are the concentrations of monomers, dimers, and detergent, K_{eq} is the equilibrium dissociation constant, and [M]/[Det] and [D]/[Det] are the concentrations of the TMD in the lipid phase. According to the described model, the dimerization process in a micellar solution is similar to the dimerization in water or in a lipidic bilayer. This model was shown to simulate the dimerization process of ErbB4 TMD in saturated lipidic bicelles, when more than one TMD is located in the same bicelle due to the low LPR [16]. In contrast, the investigation of the GpA dimerization in detergent micelles at dilute conditions revealed that the equilibrium dissociation constant demonstrates an additional dependence on the detergent concentration and may be written in the following form, which was found to be common for various detergents [13,23]:

$$K_{eq} = \frac{[M]^2}{[D]\cdot[Det]^{\gamma}}. \tag{6}$$

As an explanation of this phenomenon, the authors treated the detergent not as a solvent but as a participant of the dimerization process [13,22]. The change in the number of detergent molecules constituting the micelles during the dimerization process causes the additional dependence of the reaction kinetic parameters on the detergent concentration, which looks like the reaction has the effective order with respect to the detergent concentration (Fig. 2B):

$$\text{Monomer} + \text{Monomer} + x\cdot\text{Detergent} \leftrightarrows \text{Dimer} + y\cdot\text{Detergent},\quad \gamma = y - x,$$

[13] where x is the number of detergent molecules needed to compose two micelles with monomers and y is the number of detergent molecules needed to compose the micelle with dimer.

This model is based on the Wyman's "theory of linkage functions" [28] and performs well at high LPR [23]. In contrast, we previously reported that the behavior of the dimerization process at low LPR begins to deviate from Eq. (6) and that K_{eq} starts to decrease with an increase in the protein-to-micelle ratio [15], making this "detergent release" model inapplicable for the analysis of weakly dimerizing TMDs.

Taking into account the aforementioned results and discussion, we propose a new model for the dimerization and oligomerization processes occurring in detergent micelles, which is based on the following hypothesis:

In micellar solutions, both dimerization and dissociation occur only upon the collision and the subsequent fusion and decay of the detergent

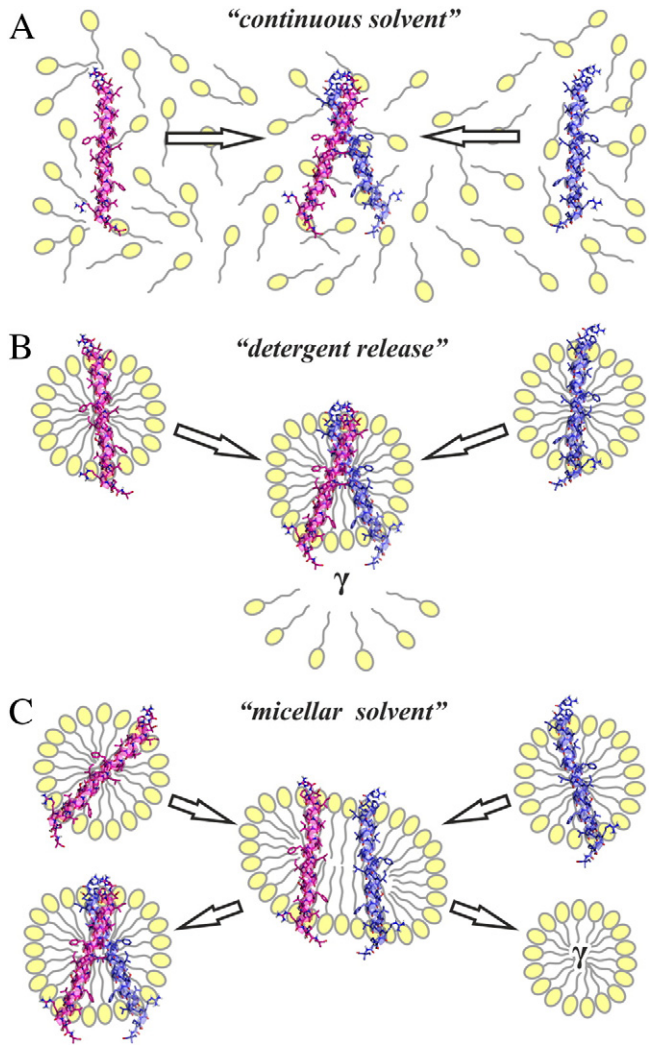

Fig. 2. Physical models considered for the dimerization process of TM helices in detergent micelles. (A) — The "continuous solvent" model, which is described by Eq. (5). (B) — The "detergent release" model, which is described by Eq. (6). (C) — The micelle-based "micellar solvent" model, which was proposed in the present work and is described by Eq. (7).

micelles. That is, two monomers will form a dimer with 100% probability once these are placed in the same micelle, and the chance of dimer (oligomer) dissociation without collision with an empty micelle is negligible. Thus, both the dimerization and the dissociation processes will be of second order (or some other order not equal to 1) with respect to detergent micelles of different types.

This assumption is the consequence of the discrete nature of the micellar solution and is based on the kinetic parameters of the dimerization processes observed in detergent micelles. Two monomers, once placed inside one micelle, will associate very fast because their possible mutual orientations and mobilities will be very limited compared with those of two monomers located in different micelles. Of course, if dimerization is unfavorable, the monomers can continuously dissociate and associate inside the micelle if the rate of the "monomolecular" dissociation is higher than the rate of collisions with empty micelles, e.g., in cases of very weak dimerization or nonspecific interactions. Thus, a single exchange peak in the NMR spectrum will be obtained if both the micelle collisions and the dimer dissociation rates are fast compared with the NMR timescale, and two sets of signals can be obtained if both processes run slowly, e.g., at a very low concentration of empty micelles. Under such conditions the dimerization/dissociation of the TM proteins inside the micelle will be observed and the described formalism cannot be applied. In other words, the expressed assumption is not only the basic hypothesis for the proposed formalism, but also determines the boundaries of the applicability of the approach. In all of the observed previously cases of TMD oligomerization ([4,15,16,29] and objects of the current work), both the dimerization and the dissociation processes are very slow (effective rates, as estimated from ZZ-exchange NMR experiments, are lower or much lower than 1 s^{-1}) and the collisions between micelles occur rather frequently ($\approx 10^6$ per second at an empty micelle concentration of 1 mM, as determined from basic diffusion theory). Therefore, in our particular case, the state with two monomers inside the same micelle is nearly negligible, and the proposed approach can be applied.

For this model, the dimerization process may be schematically represented as $\mathrm{micM} + \mathrm{micM} \rightleftarrows \mathrm{micD} + \gamma \cdot \mathrm{micE}$, where micM and micD are micelles containing a monomer and a dimer, respectively, and micE represents an empty micelle (Fig. 2C). The parameter γ now reflects the order of the dimerization with respect to the concentrations of empty micelles and was introduced to describe all of the previously reported data on the dimerization of TM helices in detergent micelles. It is noteworthy that γ is not the molecularity of the dimerization, and a fractional value of the parameter does not imply that a fractional number of empty micelles participate in the reaction. The process of dimerization in detergent solution is complex, and the effective orders of the reaction with respect to different products and reagents are the summary result of a number of the elementary reactions.

The equilibrium constant now has the following form:

$$K_{eq} = \frac{[\mathrm{micM}]^2}{[\mathrm{micD}] \cdot [\mathrm{micE}]^{\gamma}} = \frac{[M]^2}{[D] \cdot [\mathrm{micE}]^{\gamma}}, \quad [\mathrm{micE}] = \frac{[\mathrm{Det}] - \mathrm{Nm}[M] - \mathrm{Nd}[D] - \mathrm{CMC}}{\mathrm{Ne}} \tag{7}$$

where Ne, Nm, and Nd are the average numbers of detergent molecules in an empty micelle, micelles with a monomer, and micelles with a dimer, CMC is the critical micelle concentration, and $\gamma = (2\mathrm{Nm} - \mathrm{Nd})/\mathrm{Ne}$. If $[\mathrm{Det}] \gg [M] + [D]$, models (6) and (7) will be identical and yield free energies of dimerization that differ by an additive value, RT ln(Ne). However, when the LPR is low, the concentration of empty micelles will differ substantially from the overall detergent concentration, and we hypothesize that Eq. (7) will describe the behavior of the system at such conditions, which are beyond the applicability limits of the "detergent release" and "continuous solvent" models. To stress that the proposed model takes into account the micellar nature of the detergent solution, we named it the "micellar solvent" model. In general, the introduced theory treats the dimerization of TM domains as a transformation of detergent micelles, which distinguishes it from the previously published approaches that have been developed to analyze the oligomerization equilibrium of micelle-embedded proteins.

For models (5), (6), and (7), the free energy of dimerization can be obtained with the following formula:

$$\Delta G_0 = \mathrm{RT} \ln\left(K_{eq}\right), \tag{8}$$

where R is the universal gas constant, T is the ambient temperature in K and K_{eq} is the equilibrium constant.

4. Results

4.1. Analysis of the NMR spectra

Both objects under investigation exhibit slow (with subsecond–second characteristic times) oligomerization processes. In the TROSY-HSQC spectra, we observed distinct sets of cross-peaks, which correspond to the different oligomeric states of the proteins, and found that the population of the states was dependent on the LPR (Fig. 1A, B). The number of such states was two for FGFR3tm and three for VEGFR2tm.

4.2. Verification of the "micellar solvent model" for the TM helix–helix association process

The oligomerization model proposed in the theory section was first tested with FGFR3tm. For this peptide, the populations of monomeric and dimeric states were measured from the integrals of the 2D cross-peaks in a series of ^{15}N-TROSY-HSQC NMR spectra that were acquired at different LPR and detergent concentrations, as described in Section 2.3. The obtained data were used to calculate the concentrations of monomers [M] and dimers [D] of the TM domain in solution (see Section 2.4). The dependence of [M] and [D] on the detergent concentration [Det] was approximated by Eq. (7). The approximation resulted in the determination of the self-consistent parameters γ, Ne, Nm, Nd, and K_{eq}, which were found to equal 1.0 ± 0.1, 50 ± 2, 76 ± 7, 102 ± 10, and 0.10 ± 0.02, respectively (Fig. 1D). The equilibrium constant K_{eq} was used to determine the free energy of dimerization (Eq. (8)), which was found to be equal to −1.4 ± 0.3 kcal/mol.

To compare the results that were obtained from models (6) and (7), we plotted the apparent free energy of dimerization of FGRFR3tm ($\Delta G_{app} = \mathrm{RT} \ln([M]^2/[D])$, where R is the universal gas constant and T is the ambient temperature, 313 K) as a function of ln([Det]/Ne) for model (6), ln([Det]/Ne − [M] − [D]) for the simplified model (7), or ln(([Det] − Nm[M] − Nd[D])/Ne) for model (7). These three sets of processed data were supposed to demonstrate the adequacy of models (6) and (7) for the description of the observed dimerization process. In the ideal case, the data points treated with the appropriate model will lie on a straight line with a slope equal to γRT that will dissect the vertical axis at ΔG_0. As expected, the three curves were found to be linear at high LPR, whereas the curves for model (6) and the simplified model (7) ($N_m = N_d = N_e = 55$) bend at low LPR, when the concentration of detergent within the empty micelles deviates significantly from the overall detergent concentration (Fig. 3A). In other words, the analysis of the data using model (6) revealed that the dissociation constant starts to decrease at some point with a decrease in the LPR, which could be interpreted as dimerization enhancement caused by the saturation of micelles by the proteins. Processing the obtained data with model (7) yields a straight line through the whole LPR range tested, i.e., the free energy of dimerization is not affected by low LPR. In our previous works [15,16], we discarded the data points measured at low LPR. The proposed model allowed the possibility to analyze all of the data points and to significantly increase the accuracy of the interpretation and may

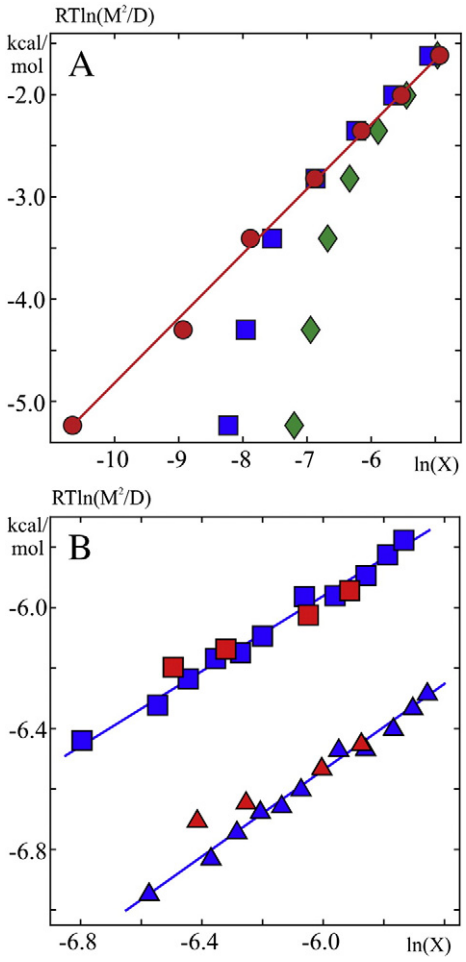

Fig. 3. (A) Apparent free energy of dimerization of FGRFR3tm $\left(\Delta G_{app} = RT \ln\left(\frac{[M]^2}{[D]}\right)\right)$ as a function of $X = RT \ln\left(\frac{[Det]}{Ne}\right)$ (lozenge), $X = RT \ln\left(\frac{[Det]}{Ne} - [M] - [D]\right)$ (square), and $X = RT \ln(([Det] - N_m[M] - N_d[D])/N_e)$ (circle). (B) Apparent free energy of dimerization of VEGFR2tm $\Delta G_{app} = RT \ln\left(\frac{[M]^2}{[D]}\right)$ as a function of the logarithm of the detergent concentration $X = RT \ln\left(\frac{[Det]}{Ne}\right)$ (triangles) or the concentration of empty micelles $X = RT \ln\left(\frac{[Det]}{Ne} - [M] - [D] - [T]\right)$ (squares). The red points were acquired at high LPR (800–1600), and the blue points correspond to a LPR of 100–400. The data points obtained with the "micellar solvent" model (squares) on panel B were shifted upward by 0.4 kcal/mol for convenience.

even provide the only possible way to measure the free energy of dimerization for weakly interacting TM helices.

The simplified model (7) yielded better results than model (6): the data points stop deviating from the straight line at lower LPR. Thus, this model can be used for the analysis of relatively stable dimers/oligomers. To test the applicability of the simplified model (7) for relatively strong dimers, we additionally processed the data for the dimerization of VEGFR2tm using the simplified model (7) and taking into account the presence of the oligomeric state (Fig. 3B). For this model, the approximation procedure can be slightly simplified: the apparent free energy of dimerization $\Delta G_{app} = RT \ln([M]^2/[D])$ was plotted as a function of the natural logarithm of the concentration of empty micelles, i.e., $\ln([Det]/55 - [M] - [D] - [O])$ ([O] is the concentration of protein in the oligomeric state, which was calculated assuming trimerization equilibrium, see Section 2.4.). These data were approximated by a linear function with slope equal to γRT that dissects the ordinate at $\Delta G_{app} = \Delta G_0$. The use of the "micellar solvent" model allowed us to improve the quality of the fit and to remove the deviations from the ideal behavior of the system that were observed when data were treated with model (6).

To conclude, the proposed model converts the populations of oligomeric states into the free energies of the oligomerization processes occurring in detergent micelles and is applicable for the investigation of weakly dimerizing TM domains that form dimers only at low LPR, which cannot be analyzed using the conventional model [22–24]. The suggested model is not a phenomenological description but relies on the physical processes that accompany the interaction of TM domains in detergent solutions.

4.3. Working with the complex equilibrium

As was stated in the introduction, the proposed technique is suitable for the analysis of a complex equilibrium, as is the case when the TM segment can remain simultaneously in more than two different populated oligomeric states. When more than two sets of cross-peaks are visible in the NMR spectrum, it is not easy to propose the model that best describes the processes occurring in the system. Three cross-peaks may correspond to various scenarios, e.g., one monomer and two dimer populations with different spatial structures, one monomer, one dimer, and one trimer populations, and one monomer, one dimer, and one tetramer populations. These equilibria cannot be distinguished based on the size, rotational, or lateral diffusion of micelle particles because the size of the micelle can be relatively large compared with the size of the associated proteins, particularly in the case of small single-span TMDs. Therefore, to obtain a complete picture of the oligomerization equilibrium, it is necessary to determine the oligomeric number for each set of cross-peaks in the NMR spectrum by studying the dependence of the populations of oligomeric states on the detergent concentration and the LPR. This analysis can be easily performed if the equilibrium constant obeys Eq. (5), but the presence of the parameter γ does not allow the differentiation between different oligomerization processes in a single detergent titration experiment. In the present work, we developed a simple protocol for this analysis and tested it with the oligomerization of VEGFR2tm. VEGFR2tm exists in three different oligomeric forms in a DPC environment, and these three forms were initially assumed to be monomer (M), dimer (D), and oligomer (O) according to the line widths of the signals in the NMR spectra. To determine the oligomeric number of O, the sample was titrated by a concentrated DPC solution, and the dependence of the apparent free energies, which were calculated for different models of the oligomerization equilibrium (dimerization, $K_{app} = [M]^2/[O]$ or $[M]^2/[D]$; trimerization, $K_{app} = [M][D]/[O]$; and tetramerization, $K_{app} = [D]^2/[O]$), on the ln(micE) was monitored. The "true" model was expected to yield a straight line in the coordinates $\{RT \ln(K_{app}), \ln(micE)\}$, whereas the use of a "false" model should result in a bended curve. Surprisingly, all four models yielded straight lines with different parameter values for ΔG_0 and γ (Fig. 4) because $\ln([M])$, $\ln([D])$, and $\ln([O])$ change linearly with $\ln([Det])$. It therefore was suggested that an abrupt change in these three concentrations will help distinguish between the alternative models. Thus, the gradual titration by DPC was followed by a twofold dilution in water and then resumed. Thus, for the "true" model, which was found to be trimerization, all of the points obtained after the dilution with water were on the same line ($\gamma = 0.95 \pm 0.1$, $\Delta G_0 = -2.9 \pm 0.2$ kcal/mol), whereas the two sets of data points obtained before and after the dilution diverged with the "false" models (Fig. 4). Additionally, for states M and D, the dimerization model also yielded a single straight line ($\gamma = 1.0 \pm 0.1$, $\Delta G_0 = -2.5 \pm 0.3$ kcal/mol), and the trimerization and tetramerization models did not.

5. Discussion

5.1. Relevance of the obtained free energies

Taking into account the complex behavior of oligomerizing TM domains in detergent micelles, the question of the relevance of the measured free energies to the processes occurring in a real biological

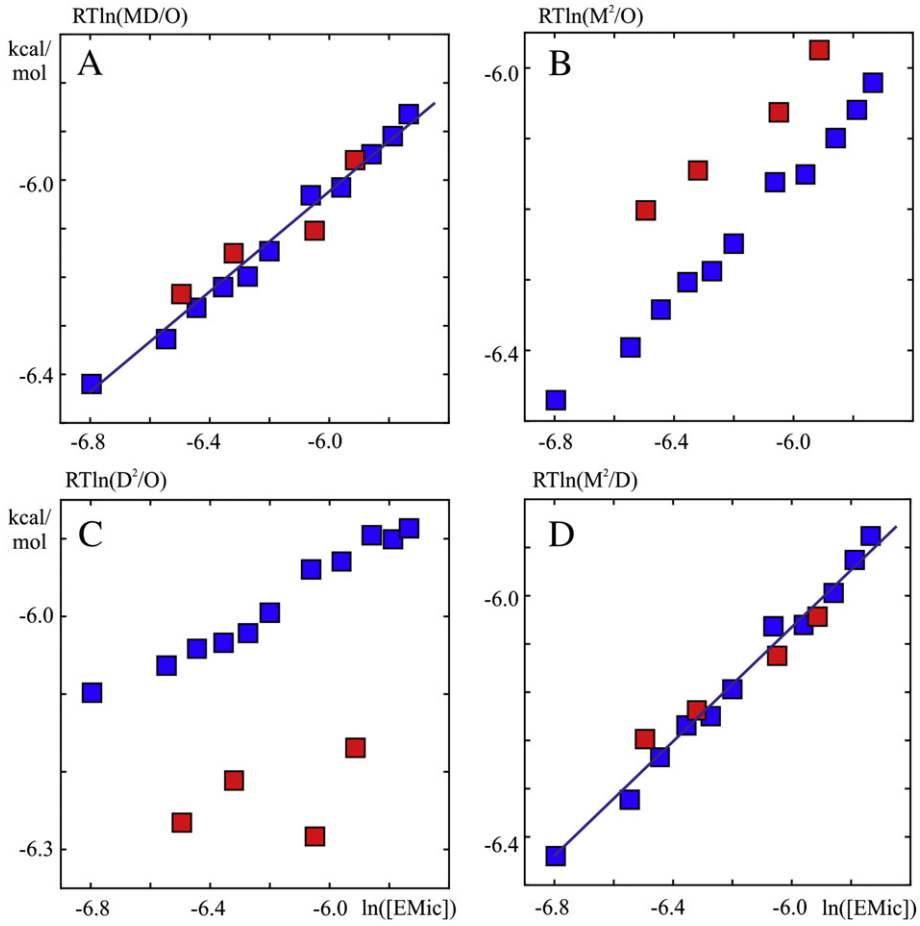

Fig. 4. Tests of the models of the oligomerization processes of VEGFR2tm in DPC micelles. The apparent free energies corresponding to trimerization (A), monomer–dimer1–dimer2 (B), tetramerization (C), or dimerization (D) equilibria are plotted as a function of the logarithm of the concentration of empty micelles. The red points were obtained after the two-fold dilution of the sample with water. The use of the proper model results in the data points forming a straight line on the plot.

system, such as a cell membrane, or even a less native system, such as model lipid bilayers, may arise. A theoretical study conducted by Zhang and Lazaridis [30] provides an approach to establish the relationship between the free energies measured in micelles and lipid bilayers in the framework of the "continuous solvent" model. This approach required calculating the loss of entropy upon the dimerization of TM peptides, taking into account the restricted mobility of TMDs in lipid bilayers and detergent micelles. The authors considered only the changes occurring with protein molecules and assumed that the detergent micelles with and without TMD(s) have the same size and structure. However, although the lipid bilayer works as a two-dimensional solvent for the TM domains, as demonstrated by all of the FRET-based experiments conducted in liposomes [27,31,32], and the dimerization of TM segments always obeys the form of Eq. (5), the dimerization or oligomerization of TM domains in micelles can be described as an interaction between large protein–detergent complexes accompanied by a rearrangement of both the protein and detergent parts. That is, the measured magnitudes of the free energy of dimerization include two terms: one of the terms represents the protein–protein and protein–detergent (lipid) interaction of the TMD, and the other arises from the collisions and exchange of matter between different detergent micelles and thus cannot be easily quantified. It therefore appears rather difficult or even impossible to find a mutual correspondence between the free energies of the dimerization of the TMDs measured in detergent micelles and the corresponding free energies in planar bilayers. Unfortunately, there are few data available for the helix–helix interactions of the same TMDs in both detergents and lipids (there is only data for GpA [24,31,33], EGFR [27,34], and FGFR3 [35]). In addition, the free energy of TM helix–helix interactions is not only affected by the type of the membrane mimetic used (e.g., micelles, bicelles, and liposomes) but also can differ significantly even for lipid bilayers of different composition [36]. Therefore, the measurements conducted in liposomes can only be employed to compare the dimerization propensity of TM domains in the same environment and do not yield accurate quantitative data that can be extrapolated to the case of a real biological system. The approach in the current work may be used for similar purposes: to compare the free energies of various TM helix–helix interactions measured in the same detergent and to find a correspondence between these thermodynamic data and the spatial structures of the dimeric membrane domains. This type of studies may yield a large amount of important information that can be used to analyze the effects of several factors, e.g., to explain the effect of single-point mutations on both the structural properties and the free energy of TM helix–helix interactions.

5.2. Advantages and drawbacks of the technique

As was mentioned previously in this manuscript, FRET, which is the most popular method for the investigation of the oligomerization of protein membrane domains in either micellar or lipidic environments, has two major drawbacks. Both are due to the inability of the approach to distinguish between specific and nonspecific interactions and between specific interactions of different types. First, this method faces difficulties with the analysis of weak dimers, which are formed only at relatively low LPR. Under such conditions, there is a high probability of unspecific contacts between the TMDs, causing fluorescence transfer and increasing the apparent dimer fraction. To overcome this problem,

one needs to correct the obtained data as described in previous studies [27,37], and this manipulation can introduce additional errors into the results. The second problem arises when the protein of interest can exist simultaneously in several oligomeric states, e.g., monomer, dimer, and trimer. In these cases, the FRET technique measures an average parameter, namely the distance between the donor and the acceptor fluorophores, and therefore cannot distinguish between the dimer and trimer states or two different dimeric states of the protein. To solve this problem, a Hill analysis [35] needs to be performed, in which the Hill coefficient describes the propensity of the TM domain to form oligomers of a higher order or alternative dimeric states. NMR spectroscopy is able to measure the structural and energetic parameters of interacting TMDs in the same experiment. If the spatial structures of a TM α-helix in the monomeric and other oligomeric states are even slightly different, these states will give rise to separate sets of cross-peaks in the NMR spectra, allowing the simultaneous detection of the populations of all states.

Nevertheless, we must acknowledge that the applicability of the introduced methodology has several limitations due to problems associated with NMR spectroscopy and general problems associated with data analysis, which are common to all other physical methods. The first limiting factor of the proposed approach is the kinetic parameters of the helix–helix interactions. The transitions between the different oligomeric forms of the TMD must be sufficiently slow to detect the separate cross-peaks, which correspond to the different states, because these sets of cross-peaks will merge into one at high kinetic rates. As we observed in our previous studies, TM helix–helix associations in micelles or bicelles commonly exhibit a slow dimer–monomer transition [6,15,16,29]. Nevertheless, it is still possible to analyze the specificity of the fast dimerization of α-helical TM segments through NMR spectroscopy, as was shown in a recent study [14], but the determination of the magnitude of the free energy of the interaction appears to be a challenging task. The second limitation is the detergent CMC (critical micelle concentration). The proposed approach, as well as all other available methods, is inapplicable for detergent concentrations below the CMC. Under these conditions, a zero concentration of both the detergent in micellar form and the detergent in empty micelles will be present in Eqs. (6) and (7). This does not correspond to the reality because the detergent will still form micellar "coats" around the TMDs. Therefore, any analysis of the data on the oligomerization of the TMD acquired below the CMC of the detergent will be senseless because the nature and properties of the protein/detergent micelles at such conditions are unknown. The third limitation of the approach is the low sensitivity of NMR spectroscopy. The working range of protein concentrations is rather low, i.e., 100 μM to 1 mM, and the minor state of the protein needs to be at least 5% of the total population for it to be detected. Furthermore, the concentration of micelles should not be very high, i.e., at a concentration of ≈500–600 mM, the detergent signals in the NMR spectra begin to markedly broaden due to an increase in the solvent viscosity and hindered rotational diffusion [38]. Therefore, the low sensitivity of NMR spectroscopy and the phenomenon of detergent CMC restricts the possible magnitudes of the LPR to a rather narrow range from ≈60–100 (aggregation number of detergent micelles) to ≈5000–6000. If no populated minor state (either monomeric in the cases of very strong dimerization or dimeric in the cases of very weak interaction) can be found under these conditions, the free energy of the dimerization cannot be obtained.

The fourth limiting factor, which is also due to the peculiarities of NMR spectroscopy as a source of data, is the size of the protein–lipid particle. Both lipid–protein nanodiscs [39] and liposomes are inapplicable for the proposed approach: liposomes are too large for solution NMR spectroscopy and nanodiscs do not allow the exchange of matter between the particles in solution [40]. Therefore, only detergent micelles and small isotropic bicelles can be used. As was stated previously, the biological relevance of the thermodynamic parameters obtained in micelles and bicelles is questionable; however, the relevance of the free energies measured through the other approaches in model lipid bilayers is also uncertain. Moreover, the usage of solution NMR spectroscopy and the application of detergent micelles allow the study of the interconnection between the spatial structure of the TMD and the free energy that characterizes the TMD dimerization because the spatial structure and the thermodynamic parameters of the TM helix–helix interactions are both investigated under the same conditions. We claim that this can be considered the main advantage of the proposed approach. The free energy of the TM helix–helix interaction measured in liposomes cannot be related to any known spatial structure of the TM domain because the identification of the spatial structure of the membrane protein in the liposome is challenging. In addition, the approach exhibits a limitation that is common to all possible physical methods. The method proposed in the current work, namely the "micellar solvent", model can be used only under conditions in which the dissociation of the dimer is much slower than the collisions of dimer-bearing micelles with empty micelles and in which a certain amount of empty micelles is present in the solution (see "Theory" section). If these conditions are not satisfied, the dimerization of TMDs inside a single micelle can be observed, and the proposed model is inapplicable. In particular, if both the collisions of micelles and the dimer dissociation are fast on the NMR timescale, the "effective" dimer population will reflect the binomial distribution of TMDs between detergent micelles, as described in a previous study [37]. However, if the dimerization/dissociation process is slow on the NMR chemical shift timescale and occurs inside a micelle (as occurs in cases with a low concentration of empty micelles), NMR can still yield some data on the thermodynamics and kinetics of the process, but a different physical model needs to be developed for the analysis of these cases.

6. Conclusion

In conclusion, a powerful technique for the investigation of the association processes of TM domains in membrane mimetics forming small particles was developed. The approach is based on the mechanistic model of the TMD oligomerization/dimerization equilibria, takes into account the fact that the dissociation of dimers/oligomers can occur only upon the collision of detergent micelles, and employs heteronuclear solution NMR spectroscopy to determine the populations of the different oligomeric states formed by the TMD. The proposed methodology can be used to study the monomer–dimer transitions in both moderately weak and strong dimers of bitopic or even polytopic membrane proteins and is applicable to the analysis of proteins that can form high-order oligomers.

Acknowledgements

This work was supported by the Russian Foundation for Basic Research (Grants 12-04-01816, 11-03-00950-a and 12-04-31027) and the Russian Academy of Sciences (Program "Molecular and Cellular Biology").

References

[1] E. Li, K. Hristova, Role of receptor tyrosine kinase transmembrane domains in cell signaling and human pathologies, Biochemistry 45 (2006) 6241–6251.
[2] E.V. Bocharov, K.S. Mineev, P.E. Volynsky, Y.S. Ermolyuk, E.N. Tkach, A.G. Sobol, V.V. Chupin, M.P. Kirpichnikov, R.G. Efremov, A.S. Arseniev, Spatial structure of the dimeric transmembrane domain of the growth factor receptor ErbB2 presumably corresponding to the receptor active state, J. Biol. Chem. 283 (2008) 6950–6956.
[3] K.R. MacKenzie, J.H. Prestegard, D.M. Engelman, A transmembrane helix dimer: structure and implications, Science 276 (1997) 131–133.
[4] E.V. Bocharov, M.L. Mayzel, P.E. Volynsky, K.S. Mineev, E.N. Tkach, Y.S. Ermolyuk, A.A. Schulga, R.G. Efremov, A.S. Arseniev, Left-handed dimer of EphA2 transmembrane domain: helix packing diversity among receptor tyrosine kinases, Biophys. J. 98 (2010) 881–889.
[5] T.-L. Lau, C. Kim, M.H. Ginsberg, T.S. Ulmer, The structure of the integrin alphaIIbbeta3 transmembrane complex explains integrin transmembrane signalling, EMBO J. 28 (2009) 1351–1361.
[6] E.V. Bocharov, M.L. Mayzel, P.E. Volynsky, M.V. Goncharuk, Y.S. Ermolyuk, A.A. Schulga, E.O. Artemenko, R.G. Efremov, A.S. Arseniev, Spatial structure and pH-dependent conformational diversity of dimeric transmembrane domain of the receptor tyrosine kinase EphA1, J. Biol. Chem. 283 (2008) 29385–29395.

[7] K.S. Mineev, E.V. Bocharov, Y.E. Pustovalova, O.V. Bocharova, V.V. Chupin, A.S. Arseniev, Spatial structure of the transmembrane domain heterodimer of ErbB1 and ErbB2 receptor tyrosine kinases, J. Mol. Biol. 400 (2010) 231–243.
[8] M.A. Lemmon, J.M. Flanagan, J.F. Hunt, B.D. Adair, B.J. Bormann, C.E. Dempsey, D.M. Engelman, Glycophorin A dimerization is driven by specific interactions between transmembrane alpha-helices, J. Biol. Chem. 267 (1992) 7683–7689.
[9] K.G. Fleming, A.L. Ackerman, D.M. Engelman, The effect of point mutations on the free energy of transmembrane alpha-helix dimerization, J. Mol. Biol. 272 (1997) 266–275.
[10] A.J. Beevers, A. Nash, M. Salazar-Cancino, D.J. Scott, R. Notman, A.M. Dixon, Effects of the oncogenic V 664 E mutation on membrane insertion, structure, and sequence-dependent interactions of the neu transmembrane domain in micelles and model membranes: an integrated biophysical and simulation study, Biochemistry 51 (2012) 2558–2568.
[11] D. Langosch, B. Brosig, H. Kolmar, H.J. Fritz, Dimerisation of the glycophorin A transmembrane segment in membranes probed with the ToxR transcription activator, J. Mol. Biol. 263 (1996) 525–530.
[12] W.P. Russ, D.M. Engelman, TOXCAT: a measure of transmembrane helix association in a biological membrane, Proc. Natl. Acad. Sci. U. S. A. 96 (1999) 863–868.
[13] L.E. Fisher, D.M. Engelman, J.N. Sturgis, Detergents modulate dimerization, but not helicity, of the glycophorin A transmembrane domain, J. Mol. Biol. 293 (1999) 639–651.
[14] T. Zhuang, B.K. Jap, C.R. Sanders, Solution NMR approaches for establishing specificity of weak heterodimerization of membrane proteins, J. Am. Chem. Soc. 133 (2011) 20571–20580.
[15] K.S. Mineev, N.F. Khabibullina, E.N. Lyukmanova, D.A. Dolgikh, M.P. Kirpichnikov, A.S. Arseniev, Spatial structure and dimer–monomer equilibrium of the ErbB3 transmembrane domain in DPC micelles, Biochim. Biophys. Acta 1808 (2011) 2081–2088.
[16] E.V. Bocharov, K.S. Mineev, M.V. Goncharuk, A.S. Arseniev, Structural and thermodynamic insight into the process of "weak" dimerization of the ErbB4 transmembrane domain by solution NMR, Biochim. Biophys. Acta 1818 (2012) 2158–2170.
[17] N.F. Khabibullina, E.N. Lyukmanova, G.S. Kopeina, Z.O. Shenkarev, A.S. Arseniev, D.A. Dolgikh, M.P. Kirpichnikov, Development and optimization of a coupled cell-free system for the synthesis of the transmembrane domain of the receptor tyrosine kinase ErbB3, Russ. J. Bioorg. Chem. 36 (2010) 603–609.
[18] D. Nietlispach, Suppression of anti-TROSY lines in a sensitivity enhanced gradient selection TROSY scheme, J. Biomol. NMR 31 (2005) 161–166.
[19] S.A. Goncharuk, M.V. Goncharuk, M.L. Mayzel, D.M. Lesovoy, V.V. Chupin, E.V. Bocharov, A.S. Arseniev, M.P. Kirpichnikov, Bacterial synthesis and purification of normal and mutant forms of human FGFR3 transmembrane segment, Acta Nat. 3 (2011) 77–84.
[20] E. Li, M. You, K. Hristova, Sodium dodecyl sulfate-polyacrylamide gel electrophoresis and forster resonance energy transfer suggest weak interactions between fibroblast growth factor receptor 3 (FGFR3) transmembrane domains in the absence of extracellular domains and ligands, Biochemistry 44 (2005) 352–360.
[21] J.H. Chill, J.M. Louis, J.L. Baber, A. Bax, Measurement of 15N relaxation in the detergent-solubilized tetrameric KcsA potassium channel, J. Biomol. NMR 36 (2006) 123–136.
[22] D. Josse, C. Ebel, D. Stroebel, A. Fontaine, F. Borges, A. Echalier, D. Baud, F. Renault, M. Le Maire, E. Chabrieres, P. Masson, Oligomeric states of the detergent-solubilized human serum paraoxonase (PON1), J. Biol. Chem. 277 (2002) 33386–33397.
[23] L.E. Fisher, D.M. Engelman, J.N. Sturgis, Effect of detergents on the association of the glycophorin a transmembrane helix, Biophys. J. 85 (2003) 3097–3105.
[24] K.G. Fleming, Standardizing the free energy change of transmembrane helix–helix interactions, J. Mol. Biol. 323 (2002) 563–571.
[25] R.A. Deems, B.R. Eaton, E.A. Dennis, Kinetic analysis of phospholipase A2 activity toward mixed micelles and its implications for the study of lipolytic enzymes, J. Biol. Chem. 250 (1975) 9013–9020.
[26] E.A. Dennis, Phospholipase A2 activity towards phosphatidylcholine in mixed micelles: surface dilution kinetics and the effect of thermotropic phase transitions, Arch. Biochem. Biophys. 158 (1973) 485–493.
[27] L. Chen, M. Merzlyakov, T. Cohen, Y. Shai, K. Hristova, Energetics of ErbB1 transmembrane domain dimerization in lipid bilayers, Biophys. J. 96 (2009) 4622–4630.
[28] J. WYMAN Jr., Linked functions and reciprocal effects in hemoglobin: a second look, Adv. Protein Chem. 19 (1964) 223–286.
[29] K.D. Nadezhdin, O.V. Bocharova, E.V. Bocharov, A.S. Arseniev, Dimeric structure of transmembrane domain of amyloid precursor protein in micellar environment, FEBS Lett. 586 (2012) 1687–1692.
[30] J. Zhang, T. Lazaridis, Calculating the free energy of association of transmembrane helices, Biophys. J. 91 (2006) 1710–1723.
[31] L. Chen, L. Novicky, M. Merzlyakov, T. Hristov, K. Hristova, Measuring the energetics of membrane protein dimerization in mammalian membranes, J. Am. Chem. Soc. 132 (2010) 3628–3635.
[32] J. Placone, K. Hristova, Direct assessment of the effect of the Gly380Arg achondroplasia mutation on FGFR3 dimerization using quantitative imaging FRET, PLoS One 7 (2012) e46678.
[33] S. Sarabipour, K. Hristova, Glycophorin A transmembrane domain dimerization in plasma membrane vesicles derived from CHO, HEK 293T, and A431 cells, Biochim. Biophys. Acta 1828 (2013) 1829–1833.
[34] J.-P. Duneau, A.P. Vegh, J.N. Sturgis, A dimerization hierarchy in the transmembrane domains of the HER receptor family, Biochemistry 46 (2007) 2010–2019.
[35] R. Soong, M. Merzlyakov, K. Hristova, Hill coefficient analysis of transmembrane helix dimerization, J. Membr. Biol. 230 (2009) 49–55.
[36] V. Anbazhagan, D. Schneider, The membrane environment modulates self-association of the human GpA TM domain—implications for membrane protein folding and transmembrane signaling, Biochim. Biophys. Acta, Biomembr. 1798 (2010) 1899–1907.
[37] F.J. Kobus, K.G. Fleming, The GxxxG-containing transmembrane domain of the CCK4 oncogene does not encode preferential self-interactions, Biochemistry 44 (2005) 1464–1470.
[38] P. Stanczak, R. Horst, P. Serrano, K. Wüthrich, NMR characterization of membrane protein–detergent micelle solutions by use of microcoil equipment, J. Am. Chem. Soc. 131 (2009) 18450–18456.
[39] I.G. Denisov, Y.V. Grinkova, A.A. Lazarides, S.G. Sligar, Directed self-assembly of monodisperse phospholipid bilayer nanodiscs with controlled size, J. Am. Chem. Soc. 126 (2004) 3477–3487.
[40] T.H. Bayburt, S.G. Sligar, Membrane protein assembly into nanodiscs, FEBS Lett. 584 (2010) 1721–1727.